RSC Advances

RSC Publishing

PAPER

View Article Online
View Journal | View Issue

Synthesis of thermally stable Ag@TiO_2 core–shell nanoprisms and plasmon–enhanced optical properties for a P3HT thin film†

Cite this: *RSC Advances*, 2013, **3**, 6016

Peng Du,[ac] Yinghui Cao,[b] Di Li,[a] Zhenyu Liu,[b] Xianggui Kong[a] and Zaicheng Sun*[a]

Received 15th November 2012,
Accepted 14th February 2013

DOI: 10.1039/c3ra22918a

www.rsc.org/advances

We develop a facile method to synthesize Ag@TiO_2 core–shell nanoprisms (NPs) with a tunable shell thickness through a simple sol–gel route. The thickness of the TiO_2 shell can be precisely tuned from 1 to 15 nm *via* changing the reaction time and amount of TiO_2 sol–gel precursor. The localized surface plasmon resonance (LSPR) absorption band shows a red-shift of over a hundred nanometers with the increasing TiO_2 shell thickness. The thermal stability of the Ag NPs is significantly improved due to the introduction of the TiO_2 shell. We investigate the enhanced absorption and fluorescence of poly(3-hexylthiophene) (P3HT) *via* coating bare Ag and Ag@TiO_2 core–shell NPs with P3HT. A similar absorption enhancement indicates that the LSPR absorption enhancement is not affected by the ultra-thin TiO_2 shell. Weak and significant fluorescence enhancements are observed for the P3HT hybrid film with bare Ag NPs and Ag@TiO_2 core–shell NPs, respectively. The bare Ag NPs work as both an enhancement element and a recombination center, which quench the P3HT fluorescence to some degree. The recombination of the charge carriers is effectively depressed by introducing the ultra-thin TiO_2 shell, which blocks the hole transfer to the Ag NPs.

Introduction

Metal nanostructures have attracted a great deal of attention during the past few decades due to their potential application in the fields of catalysis,[1,2] optics,[3–5] solar energy[6,7] and biological applications.[8–10] Surface plasmon resonance from metallic nanostructures can deliver significant control over the optical field and has a prospective utilization in light absorption enhancements in thin film solar cells.[11] Among these metal nanostructures, silver nanocrystals, in particular, exhibit a highly tunable architecture-dependent optical property known as localized surface plasmon resonance (LSPR). For example, the LSPR absorption band of Ag nanoprisms (NPs) can be continuously tuned from 350 nm to 1000 nm.[12]

During the past few years, the LSPR of metal nanoparticles has been employed in solar cells to enhance the light absorption and photocurrent generation of photovoltaic devices.[11,13–22] Recently, a 10–20% increase in the power conversion efficiency (PCE) was observed when bare Au and Ag nanoparticles were incorporated into organic photovoltaic cells. However, it is still hard to conclude that the local field enhancement from plasmon resonance is the dominant factor in the enhancement of the PCE.[15,23] Three factors, including light scattering, LSPR, and charge carrier recombination are involved in PCE enhancement. The former two factors provide a positive contribution, while carrier recombination, which involves metal nanoparticles, gives a negative effect. To avoid charge recombination centers involving metal nanoparticles, most researchers incorporated the metallic nanoparticles into a hole transfer layer of poly(3,4-ethylenedioxythiophene) poly(styrenesulfonate) (PEDOT : PSS).[16,24] Recently, Kamat *et al.* demonstrated that Ag@TiO_2 particles reduced the charge recombination between the injected electrons and the oxidized sensitizer in a photosensitization experiment.[25] Plasmon-enhanced dye-sensitized solar cells (DSSCs), involving the incorporation of Ag@TiO_2 nanoparticles into TiO_2 photoanodes, were developed and it was shown that the PCE of the DSSCs containing thin photoanodes (1.5 μm) increased from 3.1% to 4.4%.[13,26] Core–shell Ag@TiO_2 nanoparticles will be a feasible way to depress charge carrier recombination in photovoltaic devices. In previous reports, Ag@TiO_2 core–shell nanoparticles have been extensive employed as photocatalysts.[27,28] High reaction temperatures or *in situ* preparation methods were employed and resulted in a random particles size distribution and an uncontrollably thick TiO_2 shell.[27,29] In the case of the Ag NPs, a high temperature reaction results in the Ag NPs shape changing from a triangular particle into a

[a]*State Key Laboratory of Luminescence and Applications, Changchun Institute of Optics, Fine Mechanics and Physics, Chinese Academy of Sciences, 3888 East Nanhu Road, Changchun, Jilin, 130033, P. R. China. E-mail: sunzc@ciomp.ac.cn*
[b]*State Key Laboratory of Applied Optics, Changchun Institute of Optics, Fine Mechanics and Physics, Chinese Academy of Sciences, 3888 East Nanhu Road, Changchun, Jilin, 130033, P. R. China*
[c]*University of Chinese Academy of Science, 19A Yuquanlu, Beijing, 100049, P. R. China*

† Electronic supplementary information (ESI) available: more SEM, TEM, AFM images and UV-Vis spectra. See DOI: 10.1039/c3ra22918a

spherical particle which is accompanied by a blue-shift of the plasmon resonant band.[30]

It is known that the induced electric field of the surface plasmon of a metal nanoparticle strongly depends on the radial distance (10–20 nm) from the nanoparticles.[5] To maximize the LSPR enhancement, the TiO_2 shell is required to be as thin as possible. At the same time, this thin layer of TiO_2 is needed to effectively block electron–hole recombination in the Ag NPs. To the best of our knowledge, there are no reports of a facile and mild synthesis route to coat Ag NPs with a tunable ultra-thin TiO_2 layer to give enhanced optical properties. Herein, we report a facile method to prepare Ag@TiO_2 core–shell NPs through a simple sol–gel route. The thickness of the TiO_2 shell can be precisely tuned from 1 to 15 nm by varying the reaction time and the amount of TiO_2 sol–gel precursor. The corresponding LSPR absorption band of the Ag NPs shows a red-shift of over a hundred nanometers when the shell thickness is increased. The resulting Ag@TiO_2 core–shell NPs exhibited a good stability for a few months at room temperature. The LSPR enhanced absorption and fluorescence of poly(3-hexylthiophene) (P3HT) are demonstrated by depositing a P3HT thin film onto Ag@TiO_2 coated glass. An obvious fluorescence enhancement in the P3HT was observed in the presence of the Ag@TiO_2 core–shell NPs. A relative weak enhancement was obtained from the bare Ag NP/P3HT film. We deduce that the ultra-thin TiO_2 shell effectively prevents the recombination of photo-generated carriers.

Results and discussion

The preparation of the Ag@TiO_2 core–shell nanoprisms

In typical modification experiments, Ag NPs were prepared following standard literature protocols.[31] Ag@TiO_2 core–shell NPs were prepared *via* a simple sol–gel route. 10 μL of 0.7 mg mL^{-1} citric acid aqueous solution was added to 1 mL of the as-prepared Ag NPs prior to the addition of the TiO_2 sol–gel precursor. The citric anion works as a stabilizing agent to prevent the aggregation of the Ag NPs. Without the extra addition of citric acid, a white cloud was produced when the TiO_2 sol–gel precursor was added to the Ag NP solution. A non-uniform TiO_2 shell was coated onto the Ag NPs due to the rapid condensation of the TiO_2 sol–gel precursor. However, the conditions involving excess citric acid resulted in a significant blue-shift and a broadening of the plasmon resonance band (Fig. S1, ESI†). This indicates that the Ag NPs tend to form small, round particles with excess citric acid (Fig. S2†). Then 10 μL of the TiO_2 sol–gel precursor was added to the Ag NP solution. After a certain time, the Ag@TiO_2 core–shell NPs were separated by centrifugation. Generally, HCl is added to prepare the sol–gel precursor. In our case, citric acid was employed instead of HCl because HCl results in a change in the Ag NPs shape.

The TEM images shown in Fig. 1 and S3† show the as-prepared Ag NPs and the Ag NPs with TiO_2 shells of various thicknesses. The as-prepared Ag NPs contain a large population of prisms with average edge lengths and thicknesses of

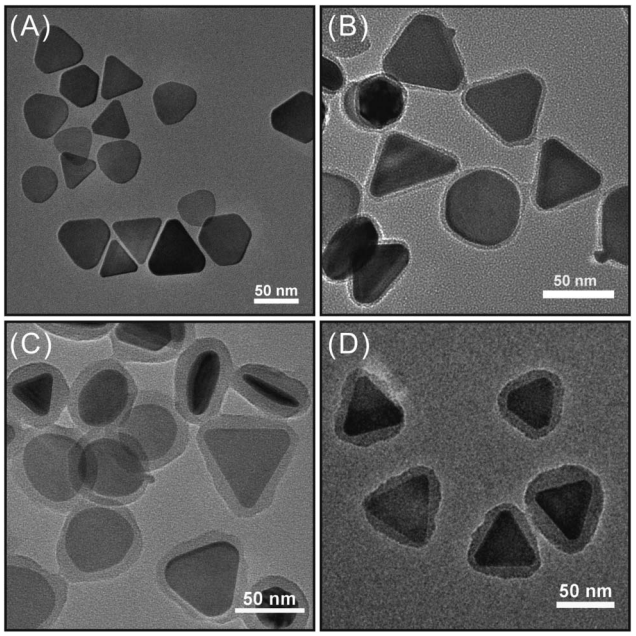

Fig. 1 TEM images of A) bare Ag NPs and Ag@TiO_2 NPs with an average shell thickness of B) 3.1 ± 0.8 nm, C) 6.7 ± 1.3 nm, and D)12.3 ± 2.12 nm.

49.4 ± 8.9 nm and 6.3 ± 0.9 nm, respectively. The UV-Vis spectrum of the as-prepared Ag NP colloid shows an intense plasmon resonant band at 698 nm (Fig. S4†). The TiO_2 coating process was monitored using UV-Vis spectroscopy by measuring the associated changes in the optical spectra of the Ag NPs after different reaction times. The resonant band of the Ag NPs immediately red-shifts ~50 nm after 15 min due to the increase of the local dielectric environment. The plasmon resonance absorption band continuously shifts to longer wavelengths when increasing the reaction time. It does not red-shift any further after 180 min. This indicates that the TiO_2 shell thickness does not increase due to the TiO_2 sol–gel precursor which might be consumed in the reaction. The TEM images indicate that 1.2 ± 0.3, 3.2 ± 0.8, and 6.7 ± 1.3 nm thick TiO_2 shells can be obtained after reaction times of 15, 60 and 180 min, respectively. TiO_2 shell thickness can also be tuned by changing the amount of the TiO_2 sol–gel precursor. The red-shift of the plasmonic resonance absorption band from 698 nm to 793, 806, 815 and 836 nm is observed in the UV-Vis spectra with the addition of 10, 20, 40 and 80 μL of the TiO_2 sol–gel precursor for 180 min (Fig. S5†). The TEM image shows that the Ag NPs were coated with ~12 nm of TiO_2 shell when 80 μL TiO_2 sol–gel precursor was added to the reaction (Fig. 1D). Ag@TiO_2 core–shell NPs in the vertical direction in the TEM image (Fig. 1C) show that the thickness of the TiO_2 shells appears uniform around all facets of the NPs. Ag@TiO_2 core–shell NPs with an ellipsoid shape are obtained by further increasing the amount of the TiO_2 sol–gel precursor and reaction time.

The plasmonic resonance absorption band of a nanoparticle is sensitive to the material composition, size, shape and local dielectric environment.[5,32] It has been previously reported that coating Au or Ag nanoparticles with a SiO_2 dielectric nanoshell

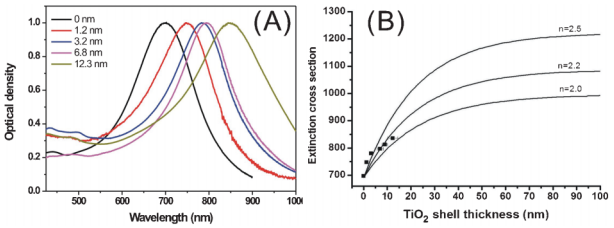

Fig. 2 (A) The normalized absorption spectra of the Ag@TiO_2 core–shell NPs before and after coating with TiO_2 shells of various thicknesses (1.2–12.3 nm). (B) A summary of the corresponding shift of the dipole plasmon resonance band as the TiO_2 shell thickness increases (square), the lines are simulation extinction cross-section maximum peaks and they increase with the shell thickness. Different values for the refractive index of the titania shell was used (marked on the line).

led to a red-shift of the nanoparticle plasmon resonance of over several tens of nanometers in wavelength, which was due to the increased refractive index (RI) of SiO_2 (1.43) in comparison to that of H_2O (1.33).[33] Here, an unexpectedly large red-shift in the plasmon resonance absorption band of Ag of over hundred nanometers in wavelength primarily occurs due to the high RI of amorphous TiO_2 (Fig. 2A). We used the numerical simulation to calculate the extinction cross-section of an individual Ag@TiO_2 NP with a fixed side length of 50 nm and a thickness of 5 nm. The RI of amorphous TiO_2 varies from 1.9 to 2.5 at 550 nm according to the preparation method.[34] The red-shift in the extinction cross-section is close to that of the experimentally fabricated NPs when the RI of amorphous TiO_2 was taken as 2.2 for the calculation (Fig. 2B). There is a little difference between the extinction cross-section and experimental results. One possible reason for this is that the synthesized samples are mixtures containing different sizes and shapes, for example, triangles, truncated triangles, and round discs. Another possible reason is that the chosen model and parameter, like the RI of TiO_2, does not match very well with the real sample.

The thermal stability of the Ag@TiO_2 core–shell nanoprisms

Recently, Xia *et al.* found that the shape of the Ag NPs changed from a shape with sharp corners to a shape with rounded corners at elevated or even room temperature.[30] As the corners of Ag NPs become gradually rounded, a gradual but significant blue-shift in the resonance peak position is observed. Later, a site-selective sulfuration method to stabilize the shape of Ag NPs was developed.[35] Ag_2S is expected to form spontaneously when elemental Ag and S_x^{2-} ions encounter each other and react in the absence of oxygen. However, it is hard to control the ratio of Ag_2S and Ag. A similar sphere-developing trend is observed in our bare Ag NP samples (Fig. S6†). An improved thermal stability is expected for the Ag@TiO_2 core–shell NPs because a layer of TiO_2 will limit the shape change in the Ag NPs. To evaluate its thermal stability, the Ag@TiO_2 core–shell NP solution is placed into an oven at 70 °C to speed up the changing process. UV-Vis spectroscopy is used to monitor the change in the plasmon resonant band. After the initial 12 h, the spectra showed no change (Fig. 3A). After longer time periods, the whole spectra shape shows no change except for a

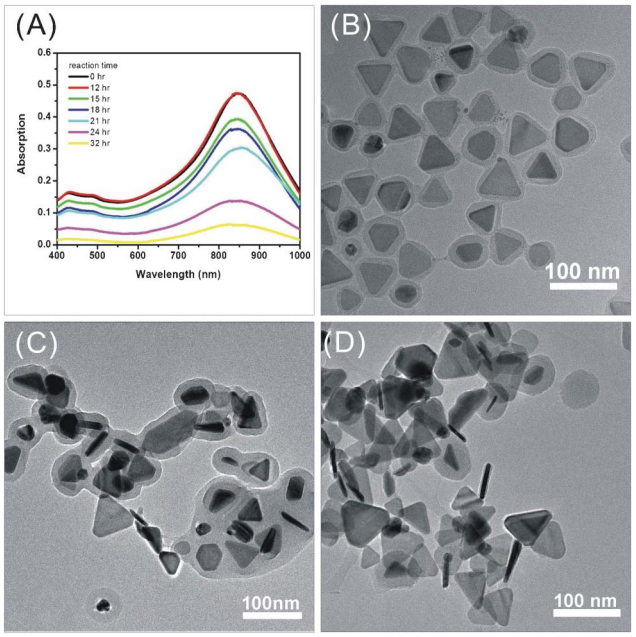

Fig. 3 UV-Vis spectra (A) of the Ag@TiO_2 solution placed in an oven at 70 °C for different time periods. TEM images of Ag@TiO_2 NPs obtained after 12 h (B), 21 h (C) and 32 h (D) at 70 °C.

decrease in the absorption intensity of the absorption bands. The color of the solution gradually turned to light blue (Fig. S7†). The TEM image (Fig. 3B) shows that after 12 h at 70 °C a uniform TiO_2 shell still covered the Ag NPs very well and the Ag@TiO_2 core–shell NPs tended to stick together. When the solution was left at 70 °C for 21 h, some of Ag@TiO_2 core–shell NPs formed big aggregates and Ag NPs that were covered with a very thin layer TiO_2 were found (Fig. 3C). The color of solution had turned to light blue. The intensity of plamonic resonant band at ~840 nm decreases to half of that of the original one. The big aggregates may not disperse very well and could precipitate from the solution due to their size. This resulted in a decrease in the concentration of the Ag@TiO_2 core–shell NPs in the solution. For the Ag@TiO_2 core–shell NPs at 70 °C for 32 h, individual Ag NPs coated with a very thick (15.0 ± 1.9 nm) or thin (1.2 ± 0.2 nm) TiO_2 layer were observed in the TEM image (Fig. 3D). The big Ag NP aggregates were not observed as they may have precipitated from the solution. However, the Ag NPs kept their shape very well, even after 32 h at 70 °C. The above results clearly indicate that the TiO_2 shell significantly improves the thermal stability of the Ag NPs. When the Ag@TiO_2 core–shell NP solution is stored at room temperature for 3 months, there is no obvious spectrum change.

The effect of LSPR on the absorption and fluorescence of a P3HT thin film

The effect of LSPR from the Ag@TiO_2 core–shell NPs on the absorption of a P3HT thin film is investigated. Ag NPs with a maximum LSPR band at ~492 nm in water are chosen in order to match the absorption band of the P3HT after the addition of the Ag NPs coated with a layer of TiO_2. The LSPR

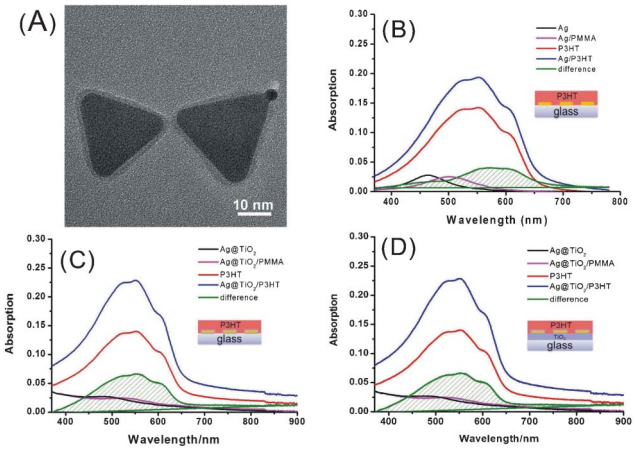

Fig. 4 The LSPR induced enhancement in absorption of the P3HT thin film. (A) TEM image of Ag@TiO_2 core–shell NPs, which are used to enhance the optical properties of P3HT. (B) The absorption spectra of bare Ag NPs (black), Ag/PMMA (purple), pure P3HT (red), Ag/P3HT (blue), and the difference (green) on bare glass. (C) The optical absorption of the Ag@TiO_2 core–shell NPs (black), Ag@TiO_2/PMMA (purple), pure P3HT (red), Ag@TiO_2/P3HT (blue), and the difference (green) on bare glass. (D) The optical absorption of the Ag@TiO_2 core–shell NPs (black), Ag@TiO_2/PMMA (purple), pure P3HT (red), Ag@TiO_2/P3HT (blue), and the difference (green) on dense TiO_2 coated glass. The difference (ΔAb) = $Ab_{NP/P3HT}$ (blue) − Ab_{P3HT} − $Ab_{NPs/PMMA}$.

band became shifted to ~500 nm after coating the Ag NPs with a TiO_2 shell with a thickness of ~2 nm (TEM image is shown in Fig. 4A). The AFM image (Fig. S8†) shows that no Ag or Ag@TiO_2 core–shell NP aggregates were observed when the NPs and P3HT are spin-coated on the substrate. In order to obtain comparable data, the optical absorption of Ag or Ag@TiO_2 core–shell NPs on the substrate have a similar absorption value (~0.025 at peak). When P3HT is coated on the NPs/substrate, the LSPR band shows a red-shift because the refractive index of the surrounding media changes from air (RI = 1.0) to P3HT (~1.9). To correct this red-shift, a PMMA thin film (RI = ~1.49) is coated on the Ag NPs/substrate. After coating with PMMA, the LSPR band of the bare Ag NPs red-shifts from 463 nm (black line in Fig. 4B) to 501 nm (purple line in Fig. 4B). The red line in Fig. 4B is the pure P3HT thin film on the bare glass. The blue line stands for the absorption of the P3HT coated Ag NPs/glass. The net enhancement of the P3HT absorption (difference spectrum, green line with shadow area) is obtained by subtracting the absorption of both pure P3HT and Ag/PMMA from the absorption of the NPs/P3HT. The absorption enhancement is calculated from the ratio of the area of the difference and the area of P3HT. An absorption enhancement of about 34% is obtained when P3HT is coated on the bare Ag NPs. The increase in the absorption of P3HT could be attributed to the interactions between the P3HT and the enhanced electric field surrounding the NPs, together with the increase of light scattering, which is also induced by LSPR and increases the optical path. The LSPR band of Ag NPs shifts from 460 nm to 487 nm after coating with a ~2 nm TiO_2 shell (Fig. 4C). This band further shifts to 526 nm after coating with PMMA. The absorption of P3HT is enhanced by ~48% due to the LSPR effect from the Ag@TiO_2 core–shell NPs when it is

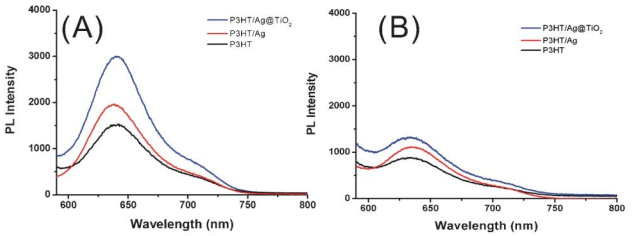

Fig. 5 The photoluminescence spectra of P3HT, the P3HT/Ag NPs and the P3HT/Ag@TiO_2 core–shell NPs on bare glass (A), and glass coated with a dense TiO_2 layer (B).

deposited on the NPs (Fig. 4C). The above results indicate that the ~2 nm thick TiO_2 shell does not affect the LSPR enhancement of the Ag NPs for P3HT. Generally, the active layer is sandwiched between the hole and electron transfer layers in solar cells. To imitate the real device, we deposited a layer of dense TiO_2 on the substrate. Fig. 4D shows the absorption spectra of the P3HT/Ag@TiO_2 on the substrate with a layer of dense TiO_2. A similar absorption enhancement (~43%) is obtained. This indicates that the absorption enhancement is maintained upon the introduction of the dense TiO_2 layer.

The absorption enhancement of P3HT is similar in all of the three situations. The next question is whether or not this absorption enhancement can be transferred into incrementing the exciton of P3HT. Generally, an increase in fluorescence intensity results in a more excited fluorophore and more exitons are produced in the same or similar sample.[36,37] When the Ag NPs are inserted underneath the P3HT thin film, an enhancement in the fluorescence of P3HT should be observed due to the LSPR of the Ag NPs. Fig. 5A shows the PL spectra of the P3HT thin film with either the bare Ag NPs or the Ag@TiO_2 core–shell NPs, and a pure P3HT thin film on the bare glass substrate. In comparison with the P3HT thin film, the fluorescence intensity increases due to the insertion of Ag or the Ag@TiO_2 NP layer. In the case of the bare Ag NPs, the LSPR has an enhancing effect on the fluorescence; on the other hand, the bare Ag NPs also quench the fluorescence because bare Ag NPs can act as a recombination center, which accepts both electrons and holes from the P3HT. These two effects cooperate in the P3HT/Ag NP hybrid film to give a relativly weak fluorescence enhancement. The fluorescence enhancement is more significant when the Ag NPs are replaced with the Ag@TiO_2 core–shell NPs. This indicates that the quenching effect is depressed by introducing the TiO_2 shell, because the hole cannot go through the TiO_2 shell and reach the Ag NPs for recombination. We also measured the PL spectra of the Ag/P3HT and Ag@TiO_2/P3HT on a dense TiO_2 layer coated glass. PL quenching is found in all cases when a layer of TiO_2 exists under the P3HT thin film (Fig. 5B). This is mainly because charge separation happens at the interface of the donor material, P3HT, and the acceptor material, the TiO_2 layer. The electron is injected from the excited P3HT into the conduction band of TiO_2. This results in the PL quenching of P3HT.

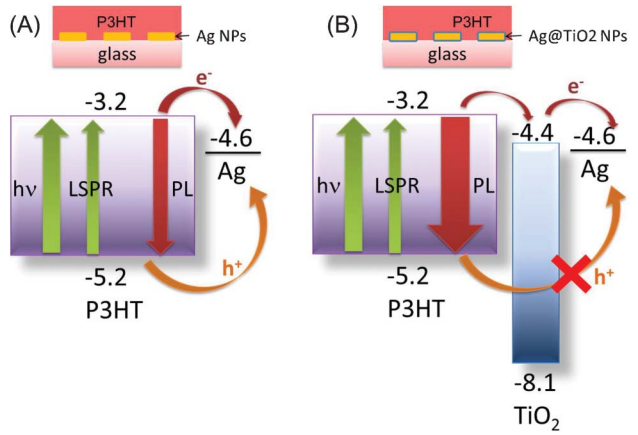

Scheme 1 Energy level diagrams of P3HT and Ag NPs referenced to the vacuum level. (A) P3HT coated bare Ag NPs. (B) P3HT coated Ag@TiO_2 core–shell NPs.

Based on the above results, we propose a Ag and Ag@TiO_2 core–shell NP LSPR enhancement mechanism. The bare Ag nanoprism works as the recombination site and enhances the fluorescence element in the hybrid film. Both photo-generated electrons and holes can inject into the bare Ag nanoprisms, where the electrons and holes can recombine together. This results in fluorescence quenching to some degree (Scheme 1A). With the TiO_2 shell, only the electrons may go through the TiO_2 shell. The photo-generated holes cannot inject into the TiO_2 shell as this is energetically forbidden. The TiO_2 shell effectively prevents the photo-generated carriers from recombining at the Ag NPs. Negative Ag NPs will inhibit further electron transfer. As a result, an enhanced fluorescence is observed (Scheme 1B).

Conclusion

In summary, we have successfully synthesized Ag@TiO_2 core–shell NPs using a simple sol–gel route. The TiO_2 shell thickness can be finely tuned from 1–15 nm through varying the reaction time and the amount of TiO_2 sol–gel precursor. The Ag@TiO_2 core–shell NPs show a good thermal stability comparing to the bare Ag NPs, and no shape changes are observed during the experimental time scale. We have studied the absorption and fluorescence enhancement of the Ag and the Ag@TiO_2 core–shell NPs on the P3HT thin film. The results show that Ag NPs with a thin TiO_2 shell layer have a similar absorption enhancement compared with the bare Ag NPs. This indicates that the TiO_2 shell does not influence the LSPR effect of the Ag NPs. PL quenching is observed when bare Ag NPs are inserted underneath the P3HT thin film because the Ag NPs are the site of the excitons recombination. Compared to the bare Ag NPs, with the Ag@TiO_2 core–shell NPs, an obvious enhanced fluorescence is observed. This indicates that the TiO_2 shell effectively blocks the recombination of excitons in the Ag NPs.

Experimental

Synthesis of Ag NPs

The Ag NPs were synthesized using a seed-mediated procedure with a few modifications.[25] In a typical synthesis of Ag seeds, aqueous trisodium citrate (22.5 mL, 2.5 mM), aqueous poly(sodium styrenesulphonate) (PSSS, 2.5 mg) and aqueous $NaBH_4$ (1.5 mL of 10 mM freshly prepared) were mixed together which was followed by the addition of aqueous $AgNO_3$ (22.5 mL, 0.5 mM) at a rate of 2 mL min^{-1} with continuous stirring. A yellow Ag seed solution was obtained for the Ag NPs preparation. 22.5 mL of ultrapure water was mixed with aqueous L-ascorbic acid (0.375 mL, 10 mM) and 0.3 mL seed solution for the synthesis of Ag NPs with a LSPR band located at 698 nm, which was followed by slow dropping of aqueous $AgNO_3$ (15 mL, 0.5 mM) at a rate of 1 mL min^{-1}. After that, aqueous trisodium citrate (2.5 mL, 25 mM) was injected to stabilize the NPs. Under magnetic stirring, the color of the solution changed gradually during the dropping of the $AgNO_3$ solution and was stable at when the solution had a blue color. The product was directly used as the Ag@TiO_2 core–shell without further purification or treatment.

Preparation of the TiO_2 sol–gel precursor

16 mg of citric acid was dissolved in 5 mL *n*-propanol, and then tributyltin (TBT) (0.34 g) was added into the above solution. After stirring for 30 min, the sol–gel precursor was filtered using a syringe filter (0.22 μm) for use in the synthesis of the Ag@TiO_2 core–shell NPs.

Synthesis of Ag@TiO_2 core–shell NPs

In a typical experiment, 1 mL of the Ag NP solution was mixed with 10 μL of 0.7 mg mL^{-1} citric acid aqueous solution, and then 10 μL of TiO_2 sol–gel solution was added with vigorous stirring (1000 rpm), with reaction times varying from 15 min to several hours. Ag@TiO_2 core–shell NPs were isolated by centrifugation at 7700 rpm for 20 min to remove excessive TiO_2 sol–gel precursor. The precipitate was redispersed in ethanol by sonication and washed two more times. Finally, the Ag@TiO_2 core–shell NPs were dispersed in ethanol solution.

Thermal stability experiments

The Ag@TiO_2 NPs ethanol solution was placed into an oven at 70 °C and aged for different time periods. Aliquots of the solution were taken out from the solution at specific times for photographs and UV-Vis extinction spectral recordings.

Enhanced absorption and fluorescence of P3HT

The glass substrate was cleaned by sonication (detergent, acetone, ethanol, water) for 20 min. The Ag or Ag@TiO_2 core–shell NPs were spin-coated on the substrate at 1000 rpm for 40 s. Then, P3HT (10 mg mL^{-1} in chlorobenzene) was spin-coated onto the Ag or Ag@TiO_2 core–shell NPs at 1000 rpm for 20 s. A dense TiO_2 layer was prepared by spin-coating the TiO_2 sol–gel precursor at 2000 rpm for 1 min on the substrate. Then the substrate was heated to 450 °C for 30 min.

Characterization

Ultraviolet-visible (UV-Vis) absorption and PL spectra were measured at room temperature using a Shimadzu UV-3101 spectrophotometer and a Hitachi F-4500, respectively. Transmission electron microscope (TEM) images were obtained using a FEI Tecnai G2 operated at 200 kV. The size of the Ag NPs and the Ag@TiO_2 core–shell NPs was obtained from TEM images by counting over 100 individual particles.

Acknowledgements

The financial support from the National Natural Science Foundation of China (No. 61071048, 61176016), the Science and Technology Department of Jilin Province (NO. 20121801) and the Returnee startup fund of Jilin is gratefully acknowledged. Z. S. and Z. L. thank the support of the ''Hundred Talent Program'' of CAS, and the Innovation and Entrepreneurship Program of Jilin.

References

1 C. T. Campbell, *Science*, 2004, **306**, 234–235.
2 M. S. Chen and D. W. Good, *Science*, 2004, **306**, 252–255.
3 W. L. Barnes, A. Dereux and T. W. Ebbesen, *Nature*, 2003, **424**, 824–830.
4 T. W. Odom and G. C. Schatz, *Chem. Rev.*, 2011, **111**, 3667–3668.
5 K. L. Kelly, E. Coronado, L. L. Zhao and G. C. Schatz, *J. Phys. Chem. B*, 2003, **107**, 668–677.
6 H. A. Atwater and A. Polman, *Nat. Mater.*, 2010, **9**, 205–213.
7 V. E. Ferry, L. A. Sweatlock, D. Pacifici and H. A. Atwater, *Nano Lett.*, 2008, **8**, 4391–4397.
8 R. Elghanian, J. J. Storhoff, R. C. Mucic, R. L. Letsinger and C. A. Mirkin, *Science*, 1997, **277**, 1078–1081.
9 A. J. Haes and R. P. Van Duyne, *J. Am. Chem. Soc.*, 2002, **124**, 10596–10604.
10 R. A. Sperling, P. Rivera Gil, F. Zhang, M. Zanella and W. J. Parak, *Chem. Soc. Rev.*, 2008, **37**, 1896.
11 M. D. Brown, T. Suteewong, R. S. S. Kumar, V. D'Innocenzo, A. Petrozza, M. M. Lee, U. Wiesner and H. J. Snaith, *Nano Lett.*, 2011, **11**, 438–445.
12 M. Rycenga, C. M. Cobley, J. Zeng, W. Li, C. H. Moran, Q. Zhang, D. Qin and Y. Xia, *Chem. Rev.*, 2011, **111**, 3669–3712.
13 J. Qi, X. Dang, P. T. Hammond and A. M. Belcher, *ACS Nano*, 2011, **5**, 7108–7116.
14 A. P. Kulkarni, K. M. Noone, K. Munechika, S. R. Guyer and D. S. Ginger, *Nano Lett.*, 2010, **10**, 1501–1505.
15 D. H. Wang, D. Y. Kim, K. W. Choi, J. H. Seo, S. H. Im, J. H. Park, O. O. Park and A. J. Heeger, *Angew. Chem., Int. Ed.*, 2011, **50**, 5519–5523.
16 D. D. S. Fung, L. Qiao, W. C. H. Choy, C. Wang, W. E. I. Sha, F. Xie and S. He, *J. Mater. Chem.*, 2011, **21**, 16349–16356.
17 Z. Zhu, H. Meng, W. Liu, X. Liu, J. Gong, X. Qiu, L. Jiang, D. Wang and Z. Tang, *Angew. Chem., Int. Ed.*, 2011, **50**, 1593–1596.
18 Y. Xia, T. D. Nguyen, M. Yang, B. Lee, A. Santos, P. Podsiadlo, Z. Tang, S. C. Glotzer and N. A. Kotov, *Nat. Nanotechnol.*, 2011, **6**, 580–587.
19 Z. Li, Z. Zhu, W. Liu, Y. Zhou, B. Han, Y. Gao and Z. Tang, *J. Am. Chem. Soc.*, 2012, **134**, 3322–3325.
20 Z. Zhu, W. Liu, Z. Li, B. Han, Y. Zhou, Y. Gao and Z. Tang, *ACS Nano*, 2012, **6**, 2326–2332.
21 J. Du, J. Qi, D. Wang and Z. Tang, *Energy Environ. Sci.*, 2012, **5**, 6914–6918.
22 Y.-H. Su, Y.-F. Ke, S.-L. Cai and Q.-Y. Yao, *Light: Sci. Appl.*, 2012, **1**, e14.
23 D. H. Wang, K. H. Park, J. H. Seo, J. Seifter, J. H. Jeon, J. K. Kim, J. H. Park, O. O. Park and A. J. Heeger, *Adv. Energy Mater.*, 2011, **1**, 766–770.
24 S.-S. Kim, S.-I. Na, J. Jo, D.-Y. Kim and Y.-C. Nah, *Appl. Phys. Lett.*, 2008, **93**, 073307.
25 P. K. Sudeep, K. Takechi and P. V. Kamat, *J. Phys. Chem. C*, 2006, **111**, 488–494.
26 H. Choi, W. T. Chen and P. V. Kamat, *ACS Nano*, 2012, **6**, 4418–4427.
27 T. Hirakawa and P. V. Kamat, *Langmuir*, 2004, **20**, 5645–5647.
28 I. Pastoriza-Santos, D. S. Koktysh, A. A. Mamedov, M. Giersig, N. A. Kotov and L. M. Liz-Marzán, *Langmuir*, 2000, **16**, 2731–2735.
29 J. Li and H. Zeng, *Angew. Chem., Int. Ed.*, 2005, **44**, 4342–4345.
30 J. Zeng, S. Roberts and Y. N. Xia, *Chem.–Eur. J.*, 2010, **16**, 12559–12563.
31 D. Aherne, D. M. Ledwith, M. Gara and J. M. Kelly, *Adv. Funct. Mater.*, 2008, **18**, 2005–2016.
32 M. R. Jones, K. D. Osberg, R. J. Macfarlane, M. R. Langille and C. A. Mirkin, *Chem. Rev.*, 2011, **111**, 3736–3827.
33 C. Xue, X. Chen, S. J. Hurst and C. A. Mirkin, *Adv. Mater.*, 2007, **19**, 4071–4074.
34 M. Zhang, G. Lin, C. Dong and L. Wen, *Surf. Coat. Technol.*, 2007, **201**, 7252–7258.
35 J. Zeng, J. Tao, D. Su, Y. Zhu, D. Qin and Y. Xia, *Nano Lett.*, 2011, **11**, 3010–3015.
36 C. D. Geddes and J. R. Lakowicz, *J. Fluoresc.*, 2002, **12**, 121–129.
37 P. P. Pompa, L. Martiradonna, A. D. Torre, F. D. Sala, L. Manna, M. De Vittorio, F. Calabi, R. Cingolani and R. Rinaldi, *Nat. Nanotechnol.*, 2006, **1**, 126–130.